Tribological synergies among chemical-modified graphene oxide nanomaterials and a phosphonium ionic liquid as additives of a biolubricant

José M. Liñeira del Río[a]*, Enriqueta R. López[a], Fátima García[b, c], Josefa Fernández[a]

[a]*Laboratory of Thermophysical and Tribological Properties, Nafomat Group, Department of Applied Physics, Faculty of Physics, University of Santiago de Compostela, 15782, Santiago de Compostela, Spain*

[b]*Centro de Investigación en Química Biolóxica e Materiais Moleculares (CIQUS), Universidade de Santiago de Compostela, 15782 Santiago de Compostela, Spain*

[c]*Departamento de Química Orgánica, Universidade de Santiago de Compostela, 15782 Santiago de Compostela, Spain*

*Corresponding author.

E-mail address: josemanuel.lineira@usc.es (José M. Liñeira del Río)

ABSTRACT: In the present work, antifriction and antiwear synergies of two functionalized graphene oxides (reduced graphene oxide, rGO, and octadecylamine-modified reduced graphene-oxide, rGO@ODA) with a phosphonium ionic liquid (IL) as additives of a biodegradable ester base oil, BIOE, were researched. For this aim, four BIOE nanodispersions were formulated: two nanodispersions without IL and two others with IL (hybrid nanolubricants), being the nanodispersions: BIOE + 0.05 wt% rGO, BIOE + 0.05 wt% rGO@ODA, BIOE + 1 wt% IL+ 0.05 wt% rGO and BIOE + 1 wt% IL+ 0.05 wt% rGO@ODA and showing all of them good temporal stability (at least 3 weeks), especially those containing the ionic liquid. Tribological assays, at pure sliding conditions, were made with the aforementioned nanolubricants and with neat BIOE under 20 N of working load. All hybrid and non-hybrid nanolubricants revealed lower coefficients of friction compared to BIOE oil, reaching a greatest friction reduction of 34% for the 1 wt% IL+ 0.05 wt% rGO nanolubricant. Discs lubricated with the prepared nanolubricants revealed smaller wear than discs lubricated with BIOE, achieving the highest wear track width reduction (34%) also for the 1 wt% IL+ 0.05 wt% rGO nanolubricant. Besides, through confocal Raman microscopy, as well as roughness analysis of tested discs, it can be assumed that surface repairing, synergetic effect and tribofilm formation mechanisms occur.

Keywords: functionalization; lubricant; nanomaterials; synergy; tribological mechanisms; tribology.

1. INTRODUCTION

One of the most important problems in science, technology and economy is planning long-term resource consumption and societal trends as well as finding an appropriate balance between them. Friction consumes around 20% of all energy used worldwide [1], while several studies show that the use of suitable lubricants could reduce the global energy consumption, greenhouse gas emissions, as well as prolonging the machinery lifespan [1,2] . According to the International Energy Agency (IEA) estimation of key technologies for reduction of CO_2 emissions, the principal impact (38%) is supposed to come from end-use energy efficiency. Additionally, the loss of lubricants is a big environmental problem: soil and water are immediately altered by lubricant system failures while the air is polluted with volatile lubricants [3]. For this purpose, it is essential to develop optimized lubricants to minimize energy losses which are also eco-friendly, reducing its environmental impact. Generally, a lubricant is composed by approximately 90 % of base oil and 10 % of additives. For this aim, in order to find the aforementioned energy and environment solutions, it is important to analyze both lubricant components.

In this vein, a possible way to design an optimal lubricant is using biodegradable oils instead of traditional mineral oils that are harmful to the environment. In fact, several authors have also emphasized the need for biodegradable lubricants to substitute traditional lubricants [4,5]. Biodegradable oils are good candidates for this purpose, nonetheless their lubricant properties are slightly worse than those of mineral oils. The use of additives can lead to significant enhancements in the tribological properties of lubricants [3]. Therefore, the use of biodegradable oils in combination with additives can yield good lubricant properties together with low environmental impact. In last years, nanotechnology and ionic liquids (ILs) are emerging as interesting alternatives to replace conventional additives which are harmful to the environment due to adverse emissions (zinc dialkyldithiophosphate, ZDDP) by less toxic additives that moreover, possess better lubricant properties due to their extraordinary physical

and chemical characteristics [6]. Specifically, nanoparticles due to their chemical stability in comparison with conventional additives are more durable [7]. Regarding ILs, Oulego et al. [8] compares environmental properties of 12 ILs potentially used as lubricant additives (phosphonium, imidazolium and ammonium cation-based ones) with two different ZDDPs. These authors observed that the tributylethylphosphonium diethylphosphate IL was the least toxic, with values of 55.2 ± 0.7 mg/L and 39.1 ± 0.6 mg/L, for *Vibrio fischeri* and *E. coli* analyses, respectively, whereas values of ZDDP1 and ZDDP2 were usually lesser than 1.0 ± 0.2 mg/L for both analyses, showing the high toxicity of these additives.

Recently, several researches [9-15] showed that adding small amounts of nanoparticles to lubricants can substantially decrease both friction and wear owing to nanoparticles can enter in the tribological place and improve the tribofilm performance [16]. Nonetheless, the key challenge in nanolubricants development is to improve their stability, as agglomerates and sediments will form in the lubricant because of van der Waals forces [17]. Hence, the compatibility of the base oil and nanoparticles is a vital issue that must be considered. For this reason, in recent years two different strategies have been addressed. The first one is to incorporate a dispersant with the nanoparticles, in order to secure their dispersion over the lubricant, and the second one is the chemical modification of the nanoparticle surface in order to achieve good compatibility with the oil chemical structure.

ILs are one of the most promising dispersants for nanoparticles since, in addition to their interesting dispersing properties [18], they also act as antifriction and anti-wear additives [19,20], exhibiting interesting positive tribological synergies with nanoparticles [21-24]. Nevertheless, research with these mixed additives (ILs and nanoparticles) for lubricants are still scarce. One of the first examples reported on graphene nanoparticles in combination with IL as lubricant additives was reported in 2017 by Sanes et al. [23] examining the tribological behavior of two oils, isoparaffinic and a fully formulated oil, additived with 1-octyl-3-methylimidazolium

tetrafluoroborate and graphene, finding positive anti-wear synergies for the former oil. Moreover, Senatore et al. [24] analyzed the tribological synergies of graphene oxide (GO) and 1-ethyl-3-methylimidazolium IL as polyalkylene glycol oil additives was described, achieving a friction decrease of 20 %.

Regarding the second strategy, surface modification of nanoparticles, there are different types attending to the method used to functionalize the nanoparticle surface [25]: reduction or oxidation [26,27], amide linkage [28,29], silanization [30,31], radical polymerization by surface-induced atom-transfer [32,33] or nanoscale ionic material, among others [34]. For instance, in a previous work [26] the tribological performance of reduced graphene oxide was analyzed as an additive to an ester base oil, finding good tribological results as well as good stability against sedimentation after the reduction of graphene oxide. Moreover, Mungse et al. [29] examined the tribological performance of a 10W-40 commercial oil additived with alkylated graphene oxide. These authors found improved stability results (up to 1 month) as well as a significantly reduction both in friction and wear in comparison to 10W-40 lubricant. Recently, Chen et al. [25] reviewed temporal stabilities of numerous nanolubricants, analyzing the different strategies to improve the stability of reported data determining that the surface modification method is vital to efficiently disperse the nanoparticles within the lubricant.

Given these above problems, it is clear that nanoparticles as lubricant additives have promising tribological properties, but there is still a problem with their stability in nanolubricants. In this work, the key objective is to examine the tribological properties of hybrid functionalized nanolubricants: reduced (rGO) and Octadecylamine-modified reduced graphene-oxide (rGO@ODA) and a phosphonium ionic liquid (tri(butyl)ethylphosphonium diethylphosphate) are used as additives of a biodegradable ester base oil (BIOE) at pure sliding conditions. To the best of our knowledge, this is the first research combining functionalized nanomaterials with the use of ionic liquids as dispersants to improve the nanolubricants stability and enhanced tribological properties.

2. Materials and methods

2.1. Materials

BIOE is a synthetic biodegradable and polymeric ester supplied by Verkol Lubricantes (Spain). BIOE oil possess a density of 0.9318 g·cm^{-3} (313.15 K), dynamic viscosity of 485.8 mPa s (313.15 K) and a 155.4 viscosity index. The BIOE oil was characterized through infrared spectroscopy (FTIR) observing the following peaks: the carbonyl stretching at 1743 cm^{-1}, a peak at 1149 cm^{-1} corresponded to the characteristic absorption of hydroxyl group and carbon–hydrogen (C- H) bending and stretching that are detected at 1459 cm^{-1} and 2921–2854 cm^{-1}, respectively [35].

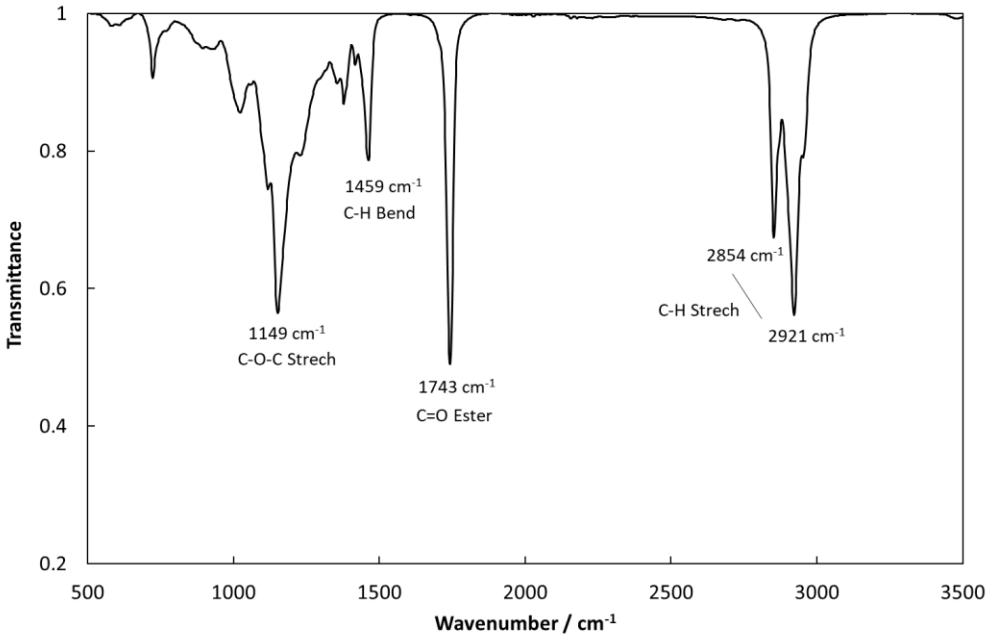

Figure 1. FTIR spectrum of BIOE base oil.

Tri(butyl)ethylphosphonium diethylphosphate ($[P_{4,4,4,2}][C_2C_2PO_4]$, CAS Number: 20445–94-7) with a purity > 95% was supplied by Iolitec (GmbH, Heilbronn, Germany) and it has a kinematic viscosity (40 °C) of 225 cSt as well as a 82 viscosity index [36]. This IL was earlier characterized by FTIR and Raman spectroscopy observing the typical band centered at 1148 cm^{-1} of the P=O stretching mode [22].

Reduced graphene oxide (rGO) nanopowders were synthesized following the Li et al. [27] procedure. For this synthesis, monolayer graphene oxide (GO), provided by Nanoninnova Technologies (Spain), was used as starting material. GO was mixed with KOH and ethanol, and then, this mix was crushed by a mortar and heated at 700 °C in a heating tube furnace. Then, the resulting nanopowder has been washed with deionized water, dried (80 °C) and after all milled in a mortar in order to decrease the size of particles. Detailed information on the experimental procedure to yield rGO can be found in a previous work [26].

Octadecylamine-modified reduced graphene-oxide (rGO@ODA) nanopowders were synthesized following the method reported by Mungse et al. [29] but using graphene oxide (GO), provided by Nanoninnova Technologies (Spain), as starting substance instead of graphite. GO nanopowders (5 g) reduction was carried out by addition of hydrazine monohydrate, (10 mL) and heating the mixture under reflux for 24 h. After letting the mixture reach room temperature the mixture was divided into two different phases: the lower one contains the precipitated rGO and the upper one is an aqueous phase. Separation of the phase containing the rGO using a separatory funnel followed by filtration through a membrane filter (0.1 um PTFE membrane) of allowed the isolation of rGO. The resulting rGO was washed by means of deionized water (45 mL) to eliminate the residual hydrazine. Afterwards, the acquired rGO powder was mildly oxidized using nitric acid, (6.25 mL, 65% purity) as oxidant, introducing carboxylic groups (-COOH) at the defect sites and edges of rGO [37]. The obtained mild oxidized rGO was refluxed in 30 mL of thionyl chloride, in the presence of 15 mL of N, N-dimethyl-formamide, converting the carboxylic groups into acyl chlorides. The residual thionyl chloride and the acylated-rGO were removed by distillation and washed with deionized water. Later, acylated-rGO powder (3.5 g) was reacted with octadecylamine (ODA), (4.5 g) under argon atmosphere at 120 °C for 4 days, achieving ODA−rGO powders through an amide linkage. The synthesized powder was dispersed and washed with ethanol (3 x 5 mL) and filtered through membrane obtaining 0.75 g of rGO@ODA.

2.2. Characterization of nanomaterials

GO, rGO and rGO@ODA nanopowders have been characterized through scanning electron microscopy (SEM) to analyze their morphology and examine the structural changes happened after GO chemical modification to produce rGO and rGO@ODA. SEM images (Fig. 2) were obtained with a Zeiss Ultraplus Field Emission Scanning Electron Microscope, FESEM. These microimages reveal that rGO sheets are partly exfoliated (Fig. 2b), in comparison to GO nanosheets (Fig. 2a). On the other hand, rGO@ODA sample (Fig. 2c) presents high aggregation level with crumpled features, this fact is owing to the absence of oxygen groups in the plane of the carbon structure sp^2 allowing ODA−rGO sheets to be connected through van der Waals forces [29].

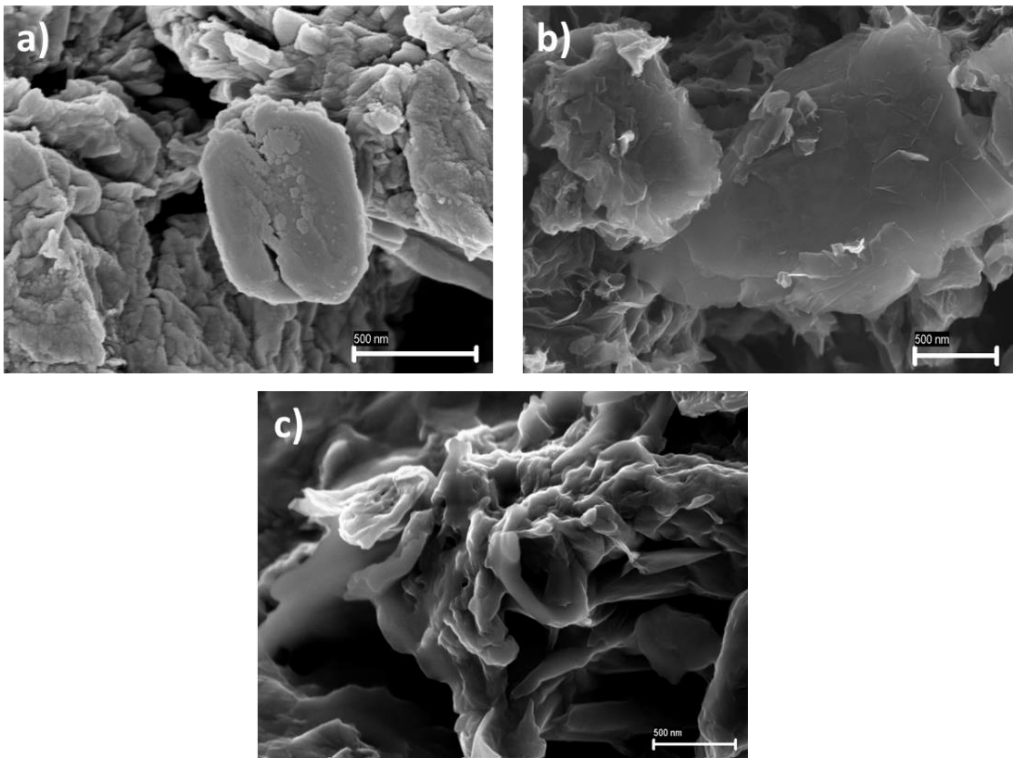

Figure 2. SEM microimages of GO (a), rGO (b), and rGO@ODA (c) nanopowders [26].

Furthermore, to confirm the successful nanopowders chemical synthesis, infrared spectroscopy (FTIR) was also used. Fig. 3 shows that GO exhibits strong absorptions bands around 3400 cm^{-1} (stretching O−H of hydroxyl groups), 1730 cm^{-1} (C=O stretch assigned to

carboxyl and carbonyl groups), 1620 cm^{-1} (C=C stretch of non-oxidized sp^2 carbon domains), 1370 cm^{-1} (bending O−H), 1250 cm^{-1} (C−O stretch associated to ether groups and phenols) and 1060 cm^{-1} (C−O stretching of hydroxyl groups) [38,39]. These vibration bands show the existence functional groups of oxygen like carbonyl, carboxyl, or hydroxyl, among others.

Regarding the rGO FTIR spectrum (Fig. 3) the bands of oxygen functional groups appear with lower intensity than in the GO spectrum, being the most important the following ones: around 1730 cm^{-1} C=O (carbonyl/carboxy) and at 1060 cm^{-1} C-O (alkoxy groups). This spectrum variation in comparison to GO spectrum implies a clear reduction of oxygen content in the rGO nanopowders.

Concerning the FTIR spectrum of rGO@ODA nanopowders [40], the addition of octadecylamine through the formation of an amide linkage is clearly verified through the presence of strong vibrational bands centered at 2915 and 2860 cm^{-1}, ascribed to the methylene (C–H) symmetric and asymmetric stretches. Likewise, as in the previous case the loss of modes of vibration related to oxygen containing groups proves the loss of oxygen functional groups as well as the restoration of the graphitic structure [28]. This fact is additional supported by strong vibrational bands around 1700 cm^{-1} (amide group C=O stretching), 1580 cm^{-1} (associated to an overlapped N−H bond and sp^2 carbon domain) and finally around 1220 cm^{-1} (stretching vibrational mode of C−N linkage) [41,42]

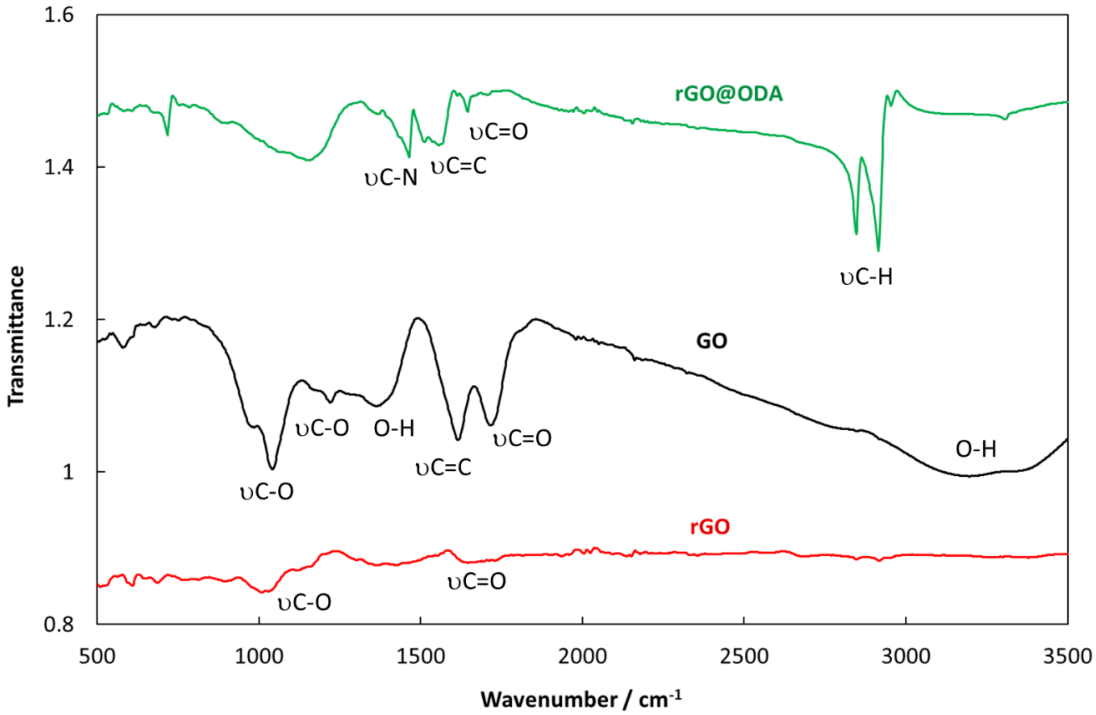

Figure 3. FTIR spectrum of GO, rGO and rGO@ODA nanopowders showing their characteristic vibrational bands.

2.3. Formulation of nanodispersions

Nanolubricants were prepared with 0.05 wt% of nanopowders (rGO and rGO@ODA) and 1 wt% of ionic liquid ($[P_{4,4,4,2}]$ $[C_2C_2PO_4]$) in the base oil (BIOE). Thus, the following nanodispersions were prepared: BIOE + (0.05 wt% rGO, 0.05 wt% rGO@ODA, BIOE +1 wt% IL+ 0.05 wt% rGO or BIOE +1 wt% IL+ 0.05 wt% rGO@ODA).

For the nanodispersions IL-free a typical two-step procedure was used: dry nanopowders were mixed with the BIOE oil using a Sartorius balance (readability of 0.01 mg) to determine the mass concentrations. Then, homogenization of the mixture performed with a bath of ultrasounds (Fisherbrand) with continuous mode during 4 h (180 W power and 37 kHz frequency). Regarding nanodispersions containing IL, a modified two-step method was used [23], instead of directly mixing nanopowders with base oil, in this case adequate amounts of rGO or rGO@ODA nanopowders were added to an agate mortar and mechanically mixed with the proper quantity of IL for 10 minutes. Afterwards, this mixture was added to the BIOE oil and homogenized as in the previous method.

2.4. Friction assays

Friction rotational assays were executed using a CSM Standard tribometer operating in ball-on-disc arrangement for the BIOE prepared nanolubricants and base oil at room temperature for: 20 N working load (1.8 GPa maximum contact pressure), 3 mm radius trajectory, distance of 340 m and speed of 10 $cm \cdot s^{-1}$. The specimens used are balls of chrome steel (AISI 52100/535A99; 3mm of radius; hardness: Rockwell Scale 58–66; Ra=0.05 μm) and stainless-steel discs (AISI52100/535A99; diameter of 10 mm; roughness of 0.02 μm (Ra) and 190–210 Hv30 hardness). Previously to each friction tests, both ball and disc have been washed in an ultrasounds bath with acetone to remove any residual material that can affect the friction tests and dried with hot air. Successively, each disc has been lubricated with around 0.2 mL of the lubricant under study. It should be noted that at least three replicates were performed to ensure a suitable repeatability. After the friction tests were completed, discs were cleaned with a hexane stream and dried with hot air being, ready to analyze the worn surface. For this aim, a 3D Sensofar S Neox Optical Profiler (confocal method, 10×) is used to quantify the wear produced on discs in terms of wear track width (WTW), wear track depth (WTD) and transversal worn area. These three wear parameters were evaluated in three separate regions of each worn track to get representative average values.

The 3D profiler is also used to determine the worn surfaces roughness (Ra) of the discs employed in friction tests to characterize the anti-wear ability of each nanolubricant. For this purpose, ISO4287 standard was used applying a Gaussian filter (cut-off: 0.08 mm wavelength).

Additionally, a Raman microscope WITec alpha300R+ was used to analyze the surface inside the worn tracks and get information about the distribution of the nanolubricants components (base oil, nanopowders and ionic liquid) on the worn surface, as well as the tribological mechanisms that take place.

3. Results and analysis

3.1. Temporal stability of nanolubricants

The temporal stability of the formulated nanolubricants has been evaluated by means of photographs. This procedure consists of analyzing the deposit of nanoparticles during time. Fig. 4 illustrates that for all nanolubricants there is no sedimentation before three weeks after the nanolubricant formulation. The observed stability is much longer than that needed to complete the friction assays (over 3 hours per each lubricant). It can also be seen from Fig. 4 that for IL-free nanolubricants, sedimentation begins to occur after four weeks. However, for hybrid nanolubricants this fact does not occur, therefore IL clearly improves the stability of the nanopowders (rGO and rGO@ODA) in the oil.

a)

Dispersion	0 day	7 days	14 days	21 days	28 days
BIOE+ 0.05wt% rGO					 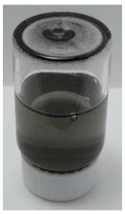
BIOE+ 0.05wt% rGO@ODA					 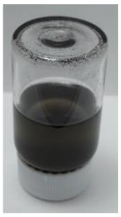

b)

Dispersion	0 day	7 days	14 days	21 days	28 days
BIOE+ 1wt% IL+ 0.05wt% rGO	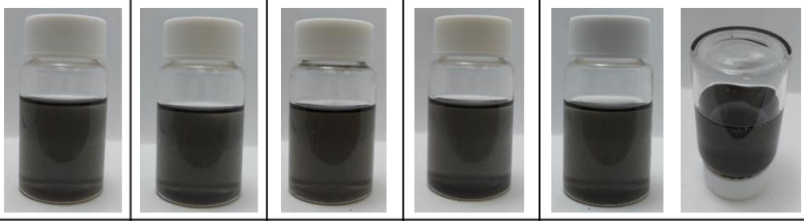				
BIOE+ 1wt% IL+ 0.05wt% rGO@ODA	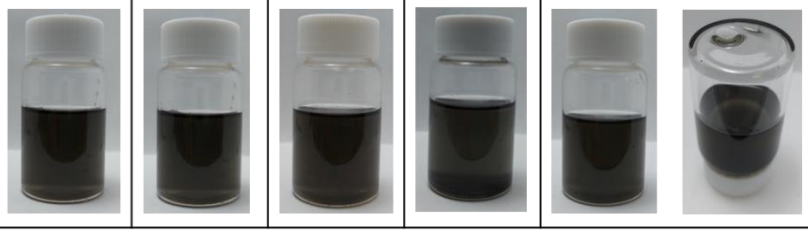				

Figure 4. Stability visual observation of BIOE nanolubricants with (b) and without (a) IL.

Likewise, refractometry was also used to study the temporal stability of the nanolubricants. The refractive index (n) of nanolubricants has been measured every hour up to 50 hours, examining its progress (Fig. 5). In a previous research [26] the n evolution of PAO 40 (or on an ester) nanolubricants additived with GO or with rGO was examined, finding that n rose over 0.4% and 0.1% for GO and rGO nanolubricants, respectively, which implies that the modification of nanoparticles improves the stability of nanolubricants. Furthermore, in other previous research [22], the progression of the n values proves an increase of over 0.1 and 0.2% for (h-BN or GnP) nanolubricants containing and non-containing IL, respectively, showing that the IL addition also improves the stability of the nanolubricants.

In the present study, the refractive index inspection of bionanolubricants (Fig. 5) reveals increases around 0.01 and 0.02 % for 1 wt% IL + 0.05 wt% rGO@ODA and for 1 wt% IL + 0.05 wt% rGO nanolubricants, respectively. Regarding the nanolubricants without IL, growths in refractive index of 0.03 and 0.06 % were obtained for 0.05 wt% rGO@ODA and for 0.05 wt% rGO nanolubricants, respectively. The achieved results reveal a great stability for the designed nanolubricants, especially in the case of nanolubricants that contain IL. Therefore, it can be

concluded that the combination of chemical modified nanopowders and the addition of IL as a dispersant is an excellent way to achieve a better stability of nanolubricants.

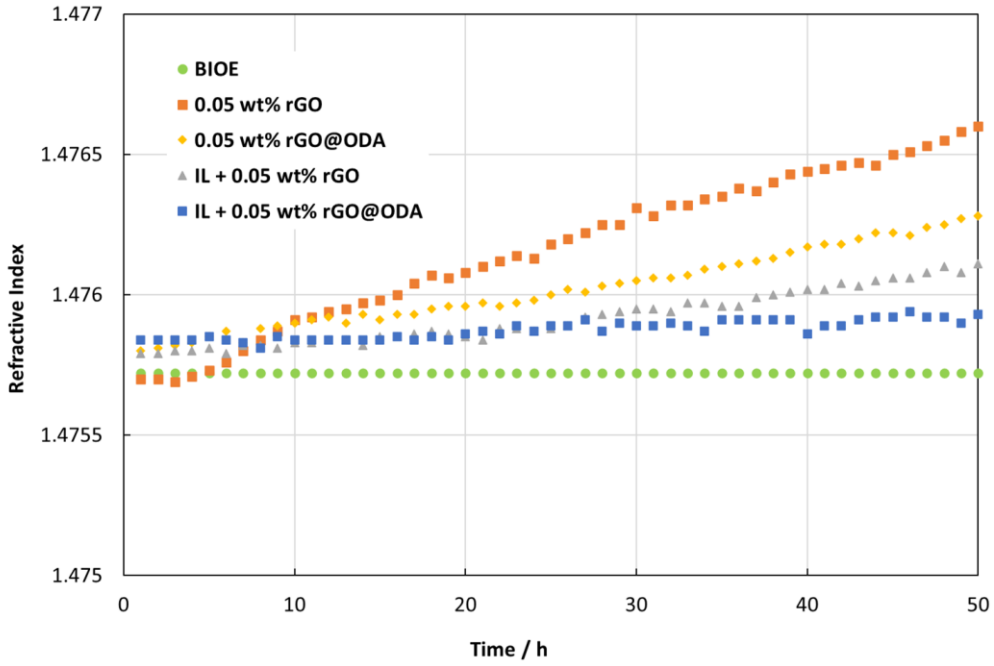

Figure 5. BIOE lubricants refractive index at 20°C versus time.

3.2. Tribological characterization

In Fig. 6 and Table 1 is showed the average coefficients of friction (μ) for the formulated BIOE nanolubricants and for the BIOE base oil. It is visibly observed that the coefficient of friction decreases considerably for all nanolubricants compared to that of BIOE base oil. Specifically, the best antifriction performance occurs for the hybrid nanolubricant BIOE+ 1 wt% IL+ 0.05 wt% rGO, showing a friction coefficient of 0.0682 versus 0.1027 attained for the non-additivated BIOE (Table 1), leading to a 34 % highest friction reduction. Regarding the other designed nanolubricants, friction reductions of 26 % (BIOE+ 1 wt% IL+ 0.05 wt% rGO@ODA), 21% (BIOE+ 0.05 wt% rGO) and 14 % (BIOE+ 0.05 wt% rGO@ODA) were achieved.

Table 1
Average coefficients of friction, μ, and average wear parameters: width (WTW), depth (WTD), and area as well as their standard deviations for the tested lubricants.

Lubricant	μ	σ	WTW/μm	σ/μm	WTD/μm	σ/μm	Area/ 10^2μm^2	σ/ 10^2μm^2
BIOE	0.1027	0.0014	271	14	1.38	0.14	2.06	0.25
+ 0.05 wt% rGO	0.0811	0.0013	239	13	0.93	0.12	1.10	0.16
+ 0.05 wt% rGO@ODA	0.0881	0.0031	244	11	1.10	0.12	1.46	0.13
+ 1 wt% IL+ 0.05 wt% rGO	0.0682	0.0010	180	10	0.61	0.11	0.59	0.17
+ 1 wt% IL+ 0.05 wt% rGO@ODA	0.0765	0.0012	196	12	0.62	0.10	0.70	0.13

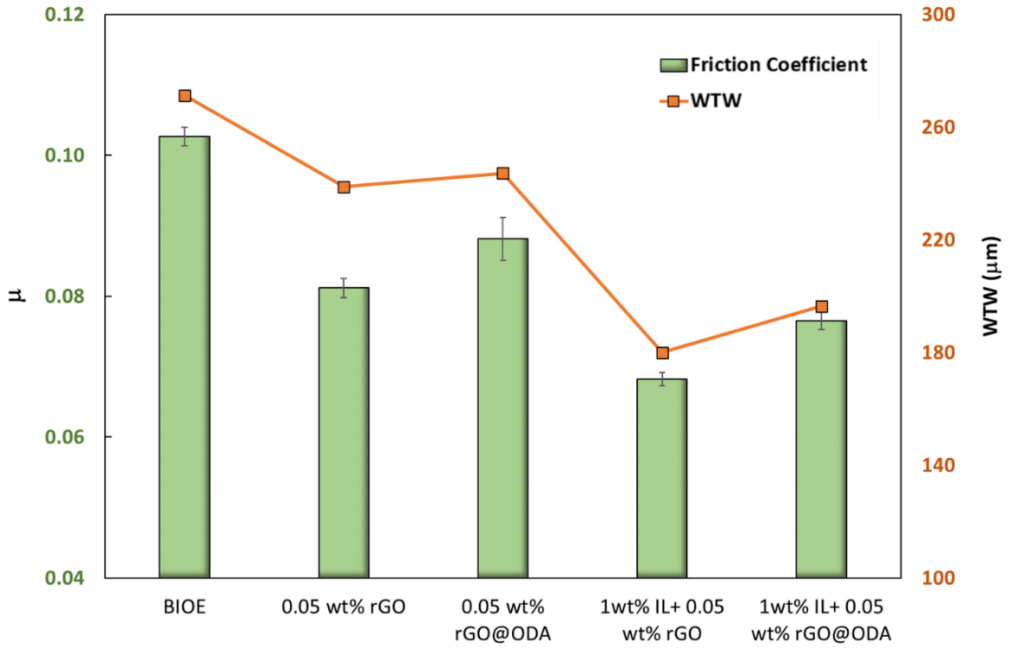

Figure 6. Comparison between the friction coefficients (μ) and the wear track widths (WTW) achieved with BIOE and BIOE nanolubricants.

Concerning the wear produced during friction tests, 3D mapping and cross-sectional profiles of worn scars in lubricated discs are displayed in Fig. 7 and Fig. 8. The WTW, WTD and cross-sectional area values found for worn tracks discs lubricated with each lubricant are presented in Table 1. It can be highlighted that for all the nanolubricants, the produced wear is less than for the BIOE base oil for all the wear parameters (WTW, WTD and area). The maximum wear decreases in width and area were achieved with the BIOE+1 wt% IL+ 0.05 wt% rGO nanolubricant, with 34 and 71 % reductions, respectively. As regards the WTD, the lowest value was obtained with the BIOE + 1 wt% IL+ 0.05 wt% rGO nanolubricant with a reduction of 56 % compared to BIOE oil.

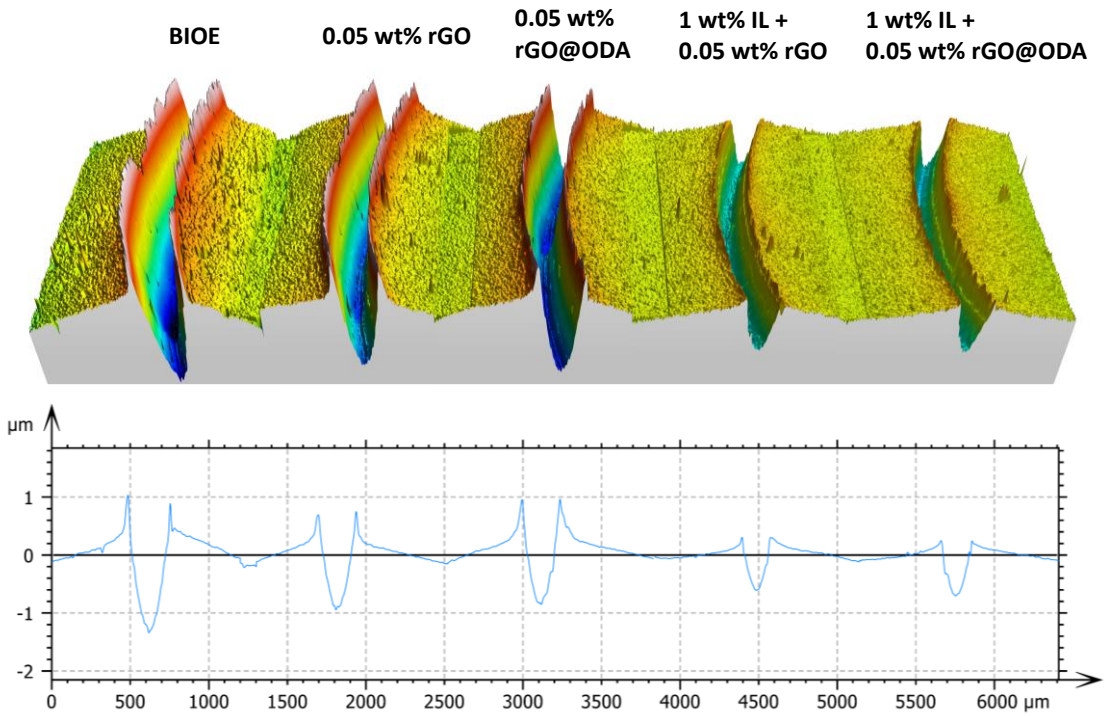

Figure 7. 3D Surface topography and worn scars cross section profiles for all the BIOE lubricants.

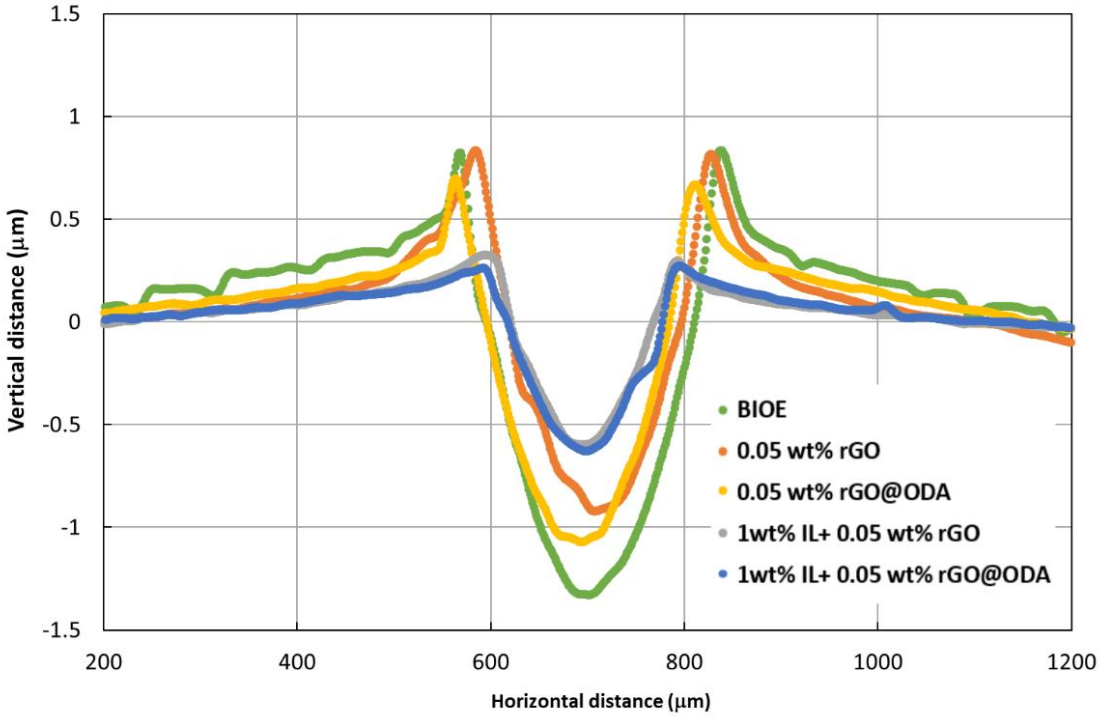

Figure 8. Cross section profiles comparison of worn scars for the BIOE lubricants.

Roughness (Ra) inside the worn disc's surfaces were examined to investigate the antiwear nanolubricants capability. Table 2 shows that worn tracks lubricated with each of the studied nanolubricants have smaller roughness than those lubricated with BIOE base oil. In particular, a Ra value of 210 nm was achieved in the BIOE worn scar while for the track lubricated

with the BIOE + 1 wt% IL+ 0.05 wt% rGO nanolubricant the tiniest Ra value (112 nm) was reached, which implies a roughness reduction of 53%.

Table 2
Values of roughness, Ra, and their uncertainties σ in the worn scars lubricated with tested BIOE nanolubricants and BIOE with a Gaussian filter (0.08 mm cut-off).

Lubricant	Ra/nm	σ
BIOE base oil	210	22
+ 0.05 wt% rGO	150	19
+ 0.05 wt% rGO@ODA	148	14
+ 1 wt% IL+ 0.05 wt% rGO	112	10
+ 1 wt% IL+ 0.05 wt% rGO@ODA	124	13

Raman spectra as also the elemental mapping of the worn scars lubricated with BIOE nanolubricants additived with rGO or rGO@ODA with or without IL were taken through a confocal Raman microscope (wavelength of 532 nm) to know the role that additives play in the wear reduction. Raman spectra of nanolubricants components (BIOE, IL, rGO and rGO@ODA) are exhibited in Figures S1-S4, respectively observing that their typical peaks agree with some of those located on the nanolubricants worn discs. Fig. 9a and Fig. 10a show a substantial presence of BIOE (blue color) and the existence of spots due to rGO and rGO@ODA nanopowders, (red color) on the worn track, especially at the edges. Concerning Figures 9b and 10b, corresponding to the discs lubricated with BIOE+IL+rGO and BIOE+IL+rGO@ODA, they illustrate the presence of BIOE (blue color), rGO or rGO@ODA nanoadditives (red color) and IL (green color) in the worn track, the additives position in worn tracks being parallel to friction sliding lines. This fact shows that nanopowders can improve the lubrication capacity of the non-additivated BIOE by producing thin tribofilms on the tribo-stressed area. In addition, van der Waals interactions between the rGO or ODA-rGO nanosheets offers low shear strength under sliding contact stress, causing a reduction in friction, whereas the constant stock of these nanomaterials on the tribological contact evades the contact between sliding surfaces and decreases the wear. Berman et al. [43] showed that 2D graphene derivatives form a protective tribofilm on the contact interfaces that provides easy shearing, resulting in friction and wear

reductions . Taking this into account and that the worn surface after tests with hybrid and non-hybrid nanolubricants of rGO or rGO@ODA are smoother than that with BIOE base oil (Table 2), as well as the corresponding Raman analyses, it can be supposed that tribological mechanisms are the tribofilms formation, as well as the repairing surface and the synergistic effects due to nanoparticles and IL.

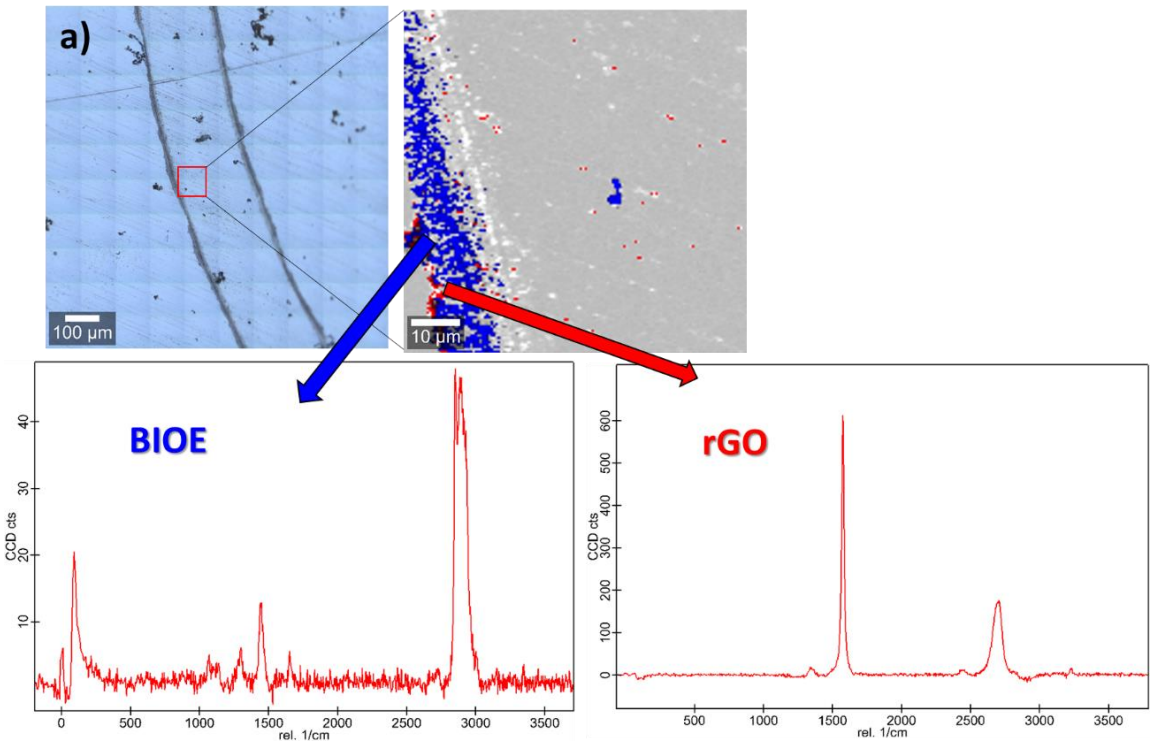

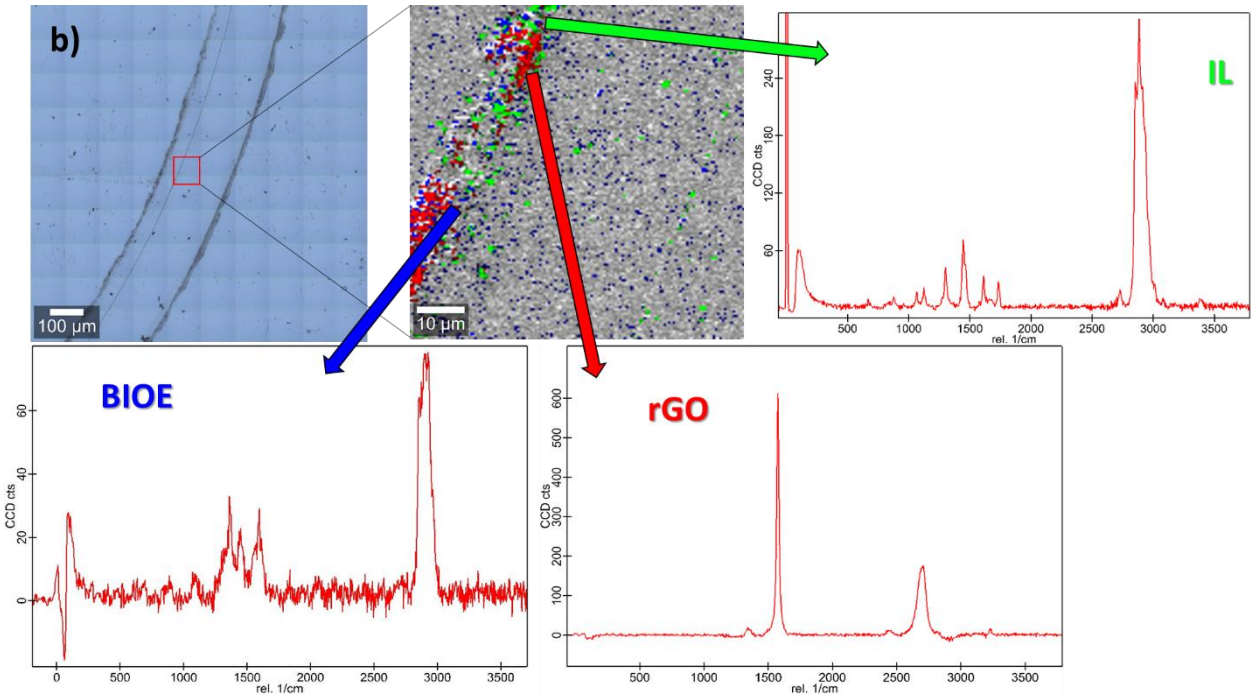

Figure 9. Elemental map and Raman spectra of worn surfaces tested with rGO nanolubricants.

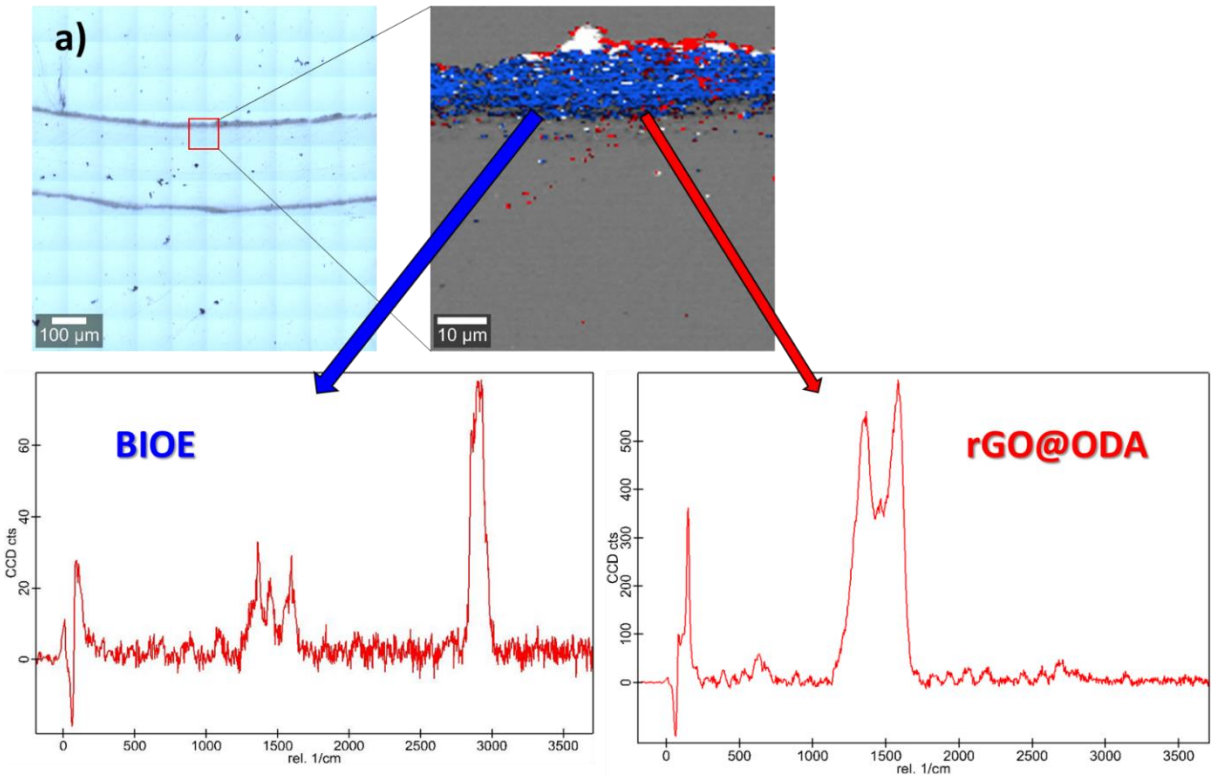

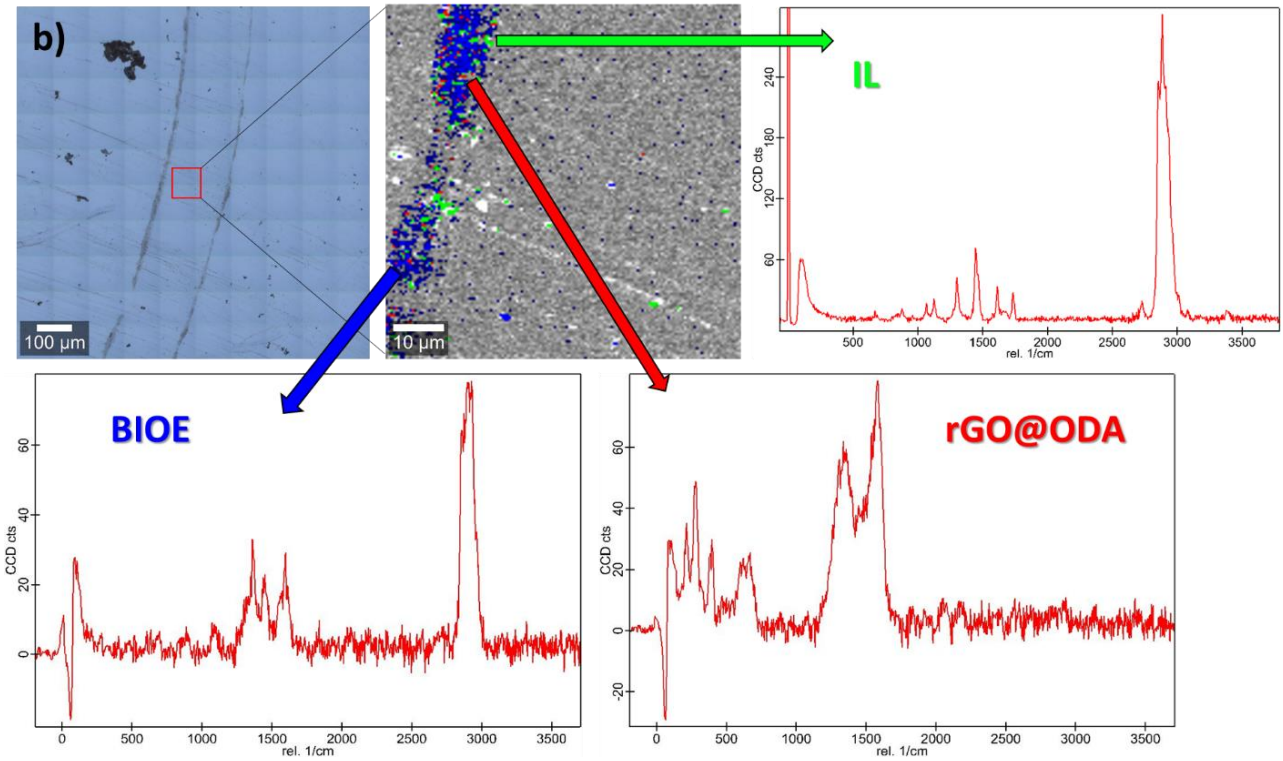

Figure 10. Elemental map and Raman spectra of worn surfaces tested with rGO@ODA nanolubricants.

4. Conclusions

In the present research the subsequent features were attained:

-Two reduced graphene oxide nanopowders, reduced graphene oxide (rGO) and octadecylamine-modified reduced graphene-oxide (rGO@ODA) have been synthesized.

-Four nanodispersions based on a biodegradable ester BIOE were prepared, two with reduced graphene oxide (rGO or rGO@ODA) NPs and two hybrid nanodispersions using an IL and rGO or rGO@ODA as additives, showing good stability times of at least three weeks.

-Friction coefficients achieved for all the nanolubricants are less than that found for the BIOE base oil, being the best friction reduction (34%) for the 1 wt% IL + 0.05 wt% rGO@ODA nanolubricant.

-For all the nanolubricants (hybrid and non-hybrid) the generated wear in the discs is lower than those for the neat BIOE in width and area. Specifically, the highest reductions were achieved for the BIOE + 1 wt% IL+ 0.05 wt% rGO nanolubricant with 34% in WTW and 71% in area.

- Through roughness and Raman studies, surface repairing, synergistic effect and formation of tribofilm mechanisms owing to the nanopowders and IL were validated.

CRediT authorship contribution statement

José M. Liñeira del Río: Writing - review & editing, Writing - original draft, Methodology, Investigation, Conceptualization. **Enriqueta R. López:** Writing - review & editing, validation, supervision, formal analysis **Fátima García**: Writing - review & editing, Methodology, Investigation **Josefa Fernández**: Writing - review & editing, Validation, Supervision, Project administration, Funding acquisition, Conceptualization.

Declaration of competing interest

None.

Acknowledgments

Authors thank Verkol Lubricantes for providing us with BIOE base oil and acknowledge the assistance of the RIAIDT-USC analytical abilities. This research was supported by Xunta de Galicia (ED431C 2020/10) and by MINECO and the ERDF programme through ENE2017-86425-C2-2-R project. FG acknowledges the Juan de la Cierva Incorporación 2017 program, the Xunta de Galicia (2016-2019, ED431G/09, Centro singular de investigación de Galicia), and Fondo Europeo de Desarrollo Regional (FEDER) for financial support.

REFERENCES

[1] K. Holmberg, A. Erdemir, The impact of tribology on energy use and CO2 emission globally and in combustion engine and electric cars, Tribology International 135 (2019) 389-396. https://doi.org/10.1016/j.triboint.2019.03.024

[2] K. Holmberg, A. Erdemir, Influence of tribology on global energy consumption, costs and emissions, Friction 5 (2017) 263-284. https://doi.org/10.1007/s40544-017-0183-5

[3] S.P. Darminesh, N.A.C. Sidik, G. Najafi, R. Mamat, T.L. Ken, Y. Asako, Recent development on biodegradable nanolubricant: A review, International Communications in Heat and Mass Transfer 86 (2017) 159-165. https://doi.org/10.1016/j.icheatmasstransfer.2017.05.022

[4] S. Rani, M.L. Joy, K.P. Nair, Evaluation of physiochemical and tribological properties of rice bran oil – biodegradable and potential base stoke for industrial lubricants, Industrial Crops and Products 65 (2015) 328-333. https://doi.org/10.1016/j.indcrop.2014.12.020

[5] I.S. Tamada, P.R.M. Lopes, R.N. Montagnolli, E.D. Bidoia, Biodegradation and toxicological evaluation of lubricant oils %J Brazilian Archives of Biology and Technology, 55 (2012) 951-956. http://dx.doi.org/10.1590/S1516-89132012000600020

[6] L. Peña-Parás, J. Taha-Tijerina, L. Garza, D. Maldonado-Cortés, R. Michalczewski, C. Lapray, Effect of CuO and Al2O3 nanoparticle additives on the tribological behavior of fully formulated oils, Wear 332-333 (2015) 1256-1261. https://doi.org/10.1016/j.wear.2015.02.038

[7] H. Spikes, Friction Modifier Additives, Tribology Letters 60 (2015) 5. https://doi.org/10.1007/s11249-015-0589-z

[8] P. Oulego, D. Blanco, D. Ramos, J.L. Viesca, M. Díaz, A. Hernández Battez, Environmental properties of phosphonium, imidazolium and ammonium cation-based ionic liquids as potential lubricant additives, Journal of Molecular Liquids 272 (2018) 937-947. https://doi.org/10.1016/j.molliq.2018.10.106

[9] A. Singh, P. Chauhan, T.G. Mamatha, A review on tribological performance of lubricants with nanoparticles additives, Materials Today: Proceedings 25 (2020) 586-591. https://doi.org/10.1016/j.matpr.2019.07.245

[10] S. Shahnazar, S. Bagheri, S.B. Abd Hamid, Enhancing lubricant properties by nanoparticle additives, International Journal of Hydrogen Energy 41 (2016) 3153-3170. https://doi.org/10.1016/j.ijhydene.2015.12.040

[11] G. Paul, H. Hirani, T. Kuila, N.C. Murmu, Nanolubricants dispersed with graphene and its derivatives: an assessment and review of the tribological performance, Nanoscale 11 (2019) 3458-3483. https://doi.org/10.1039/C8NR08240E

[12] A. Kotia, P. Rajkhowa, G.S. Rao, S.K. Ghosh, Thermophysical and tribological properties of nanolubricants: A review, Heat and Mass Transfer 54 (2018) 3493-3508. https://doi.org/10.1007/s00231-018-2351-1

[13] W.K. Shafi, M.S. Charoo, An overall review on the tribological, thermal and rheological properties of nanolubricants, Tribology - Materials, Surfaces & Interfaces 15 (2021) 20-54. https://doi.org/10.1080/17515831.2020.1785233

[14] A. Hernández Battez, R. González, J.L. Viesca, J.E. Fernández, J.M. Díaz Fernández, A. Machado, R. Chou, J. Riba, CuO, ZrO_2 and ZnO nanoparticles as antiwear additive in oil lubricants, Wear 265 (2008) 422-428. https://doi.org/10.1016/j.wear.2007.11.013

[15] A. Hernandez Battez, J.E. Fernandez Rico, A. Navas Arias, J.L. Viesca Rodriguez, R. Chou Rodriguez, J.M. Diaz Fernandez, The tribological behaviour of ZnO nanoparticles as an additive to PAO6, Wear 261 (2006) 256-263. https://doi.org/10.1016/j.wear.2005.10.001

[16] A.V. Bondarev, A. Fraile, T. Polcar, D.V. Shtansky, Mechanisms of friction and wear reduction by h-BN nanosheet and spherical W nanoparticle additives to base oil: Experimental study and molecular dynamics simulation, Tribology International 151 (2020) 106493. https://doi.org/10.1016/j.triboint.2020.106493

[17] D.K. Devendiran, V.A. Amirtham, A review on preparation, characterization, properties and applications of nanofluids, Renewable and Sustainable Energy Reviews 60 (2016) 21-40. https://doi.org/10.1016/j.rser.2016.01.055

[18] V. Khare, M.-Q. Pham, N. Kumari, H.-S. Yoon, C.-S. Kim, J.-I.L. Park, S.-H. Ahn, Graphene–Ionic Liquid Based Hybrid Nanomaterials as Novel Lubricant for Low Friction and Wear, ACS Applied Materials & Interfaces 5 (2013) 4063-4075. https://doi.org/10.1021/am302761c

[19] Y. Zhou, J. Qu, Ionic Liquids as Lubricant Additives: A Review, ACS Applied Materials & Interfaces 9 (2017) 3209-3222. https://doi.org/10.1021/acsami.6b12489

[20] M. Cai, Q. Yu, W. Liu, F. Zhou, Ionic liquid lubricants: when chemistry meets tribology, Chemical Society Reviews 49 (2020) 7753-7818. https://doi.org/10.1039/D0CS00126K

[21] K.I. Nasser, J.M. Liñeira del Río, E.R. López, J. Fernández, Synergistic effects of hexagonal boron nitride nanoparticles and phosphonium ionic liquids as hybrid lubricant additives, Journal of Molecular Liquids 311 (2020) 113343. https://doi.org/10.1016/j.molliq.2020.113343

[22] J.M. Liñeira del Río, E.R. López, J. Fernández, Synergy between boron nitride or graphene nanoplatelets and tri(butyl)ethylphosphonium diethylphosphate ionic liquid as lubricant additives of triisotridecyltrimellitate oil, Journal of Molecular Liquids 301 (2020) 112442. https://doi.org/10.1016/j.molliq.2020.112442

[23] J. Sanes, M.-D. Avilés, N. Saurín, T. Espinosa, F.-J. Carrión, M.-D. Bermúdez, Synergy between graphene and ionic liquid lubricant additives, Tribology International 116 (2017) 371-382. https://doi.org/10.1016/j.triboint.2017.07.030

[24] A. Senatore, M. Pisaturo, D. Guida, Polyalkylene glycol based lubricants and tribological behaviour: Role of ionic liquids and graphene oxide as additives, Journal of Nanoscience and Nanotechnology 18 (2018) 913-924. https://doi.org/10.1166/jnn.2018.15253

[25] Y. Chen, P. Renner, H. Liang, Dispersion of Nanoparticles in Lubricating Oil: A Critical Review, 7 (2019) 7. https://doi.org/10.3390/lubricants7010007

[26] J.M. Liñeira del Río, E.R. López, J. Fernández, F. García, Tribological properties of dispersions based on reduced graphene oxide sheets and trimethylolpropane trioleate or PAO 40 oils, Journal of Molecular Liquids 274 (2019) 568-576. https://doi.org/10.1016/j.molliq.2018.10.107

[27] Y. Li, J. Zhao, T. Cheng, Y. He, Y. Wang, J. Chen, J. Mao, Q. Zhou, B. Wang, F. Wei, J. Luo, G. Shi, Highly Exfoliated Reduced Graphite Oxide Powders as Efficient Lubricant Oil Additives, Advanced Materials Interfaces 3 (2016) 1600700. https://doi.org/10.1002/admi.201600700

[28] H.P. Mungse, N. Kumar, O.P. Khatri, Synthesis, dispersion and lubrication potential of basal plane functionalized alkylated graphene nanosheets, RSC Advances 5 (2015) 25565-25571. https://doi.org/10.1039/C4RA16975A

[29] H.P. Mungse, O.P. Khatri, Chemically Functionalized Reduced Graphene Oxide as a Novel Material for Reduction of Friction and Wear, The Journal of Physical Chemistry C 118 (2014) 14394-14402. https://doi.org/10.1021/jp5033614

[30] C. Shahar, D. Zbaida, L. Rapoport, H. Cohen, T. Bendikov, J. Tannous, F. Dassenoy, R. Tenne, Surface Functionalization of WS2 Fullerene-like Nanoparticles, Langmuir 26 (2010) 4409-4414. https://doi.org/10.1021/la903459t

[31] S. Kumari, O.P. Sharma, R. Gusain, H.P. Mungse, A. Kukrety, N. Kumar, H. Sugimura, O.P. Khatri, Alkyl-Chain-Grafted Hexagonal Boron Nitride Nanoplatelets as Oil-Dispersible Additives for Friction and Wear Reduction, ACS Applied Materials & Interfaces 7 (2015) 3708-3716. https://doi.org/10.1021/am5083232

[32] R. Wright, K. Wang, J. Qu, B. Zhao, Oil-Soluble Polymer Brush-Grafted Nanoparticles as Effective Lubricant Additives for Friction and Wear Reduction, Angewandte Chemie 128 (2016). https://doi.org/10.1002/ange.201603663

[33] B. Seymour, R. Wright, A. Parrott, H. Gao, A. Martini, J. Qu, S. Dai, B. Zhao, Poly(alkyl methacrylate) Brush-Grafted Silica Nanoparticles as Oil Lubricant Additives: Effects of Alkyl Pendant Group on Oil Dispersibility, Stability, and Lubrication Property, ACS Applied Materials & Interfaces 9 (2017). https://doi.org/10.1021/acsami.7b06714

[34] J. Yang, Y. Xia, H. Song, B. Chen, Z. Zhang, Synthesis of the liquid-like graphene with excellent tribological properties, Tribology International 105 (2017) 118-124. https://doi.org/10.1016/j.triboint.2016.09.040

[35] Y. Wu, W. Li, M. Zhang, X. Wang, Improvement of oxidative stability of trimethylolpropane trioleate lubricant, Thermochimica Acta 569 (2013) 112-118. https://doi.org/10.1016/j.tca.2013.05.033

[36] I. Otero, E.R. López, M. Reichelt, M. Villanueva, J. Salgado, J. Fernández, Ionic Liquids Based on Phosphonium Cations As Neat Lubricants or Lubricant Additives for a Steel/Steel Contact, ACS Applied Materials & Interfaces 6 (2014) 13115-13128. https://doi.org/10.1021/am502980m

[37] J. Zhang, H. Zou, Q. Qing, Y. Yang, Q. Li, Z. Liu, X. Guo, Z. Du, Effect of Chemical Oxidation on the Structure of Single-Walled Carbon Nanotubes, The Journal of Physical Chemistry B 107 (2003) 3712-3718. https://doi.org/10.1021/jp027500u

[38] M. Acik, G. Lee, C. Mattevi, A. Pirkle, R.M. Wallace, M. Chhowalla, K. Cho, Y. Chabal, The Role of Oxygen during Thermal Reduction of Graphene Oxide Studied by Infrared Absorption Spectroscopy, The Journal of Physical Chemistry C 115 (2011) 19761-19781. https://doi.org/10.1021/jp2052618

[39] C. Su, M. Acik, K. Takai, J. Lu, S.-j. Hao, Y. Zheng, P. Wu, Q. Bao, T. Enoki, Y.J. Chabal, K. Ping Loh, Probing the catalytic activity of porous graphene oxide and the origin of this behaviour, Nature Communications 3 (2012) 1298. https://doi.org/10.1038/ncomms2315

[40] T. Bao, Z. Wang, Y. Zhao, Y. Wang, X. Yi, Composition, Structure and Morphology Evolution of Octadecylamine (ODA)⁻Reduced Graphene Oxide and Its Dispersion Stability under Different Reaction Conditions, Materials (Basel) 11 (2018) 1710. https://doi.org/10.3390/ma11091710

[41] S. Choudhary, H.P. Mungse, O.P. Khatri, Dispersion of alkylated graphene in organic solvents and its potential for lubrication applications, Journal of Materials Chemistry 22 (2012) 21032-21039. https://doi.org/10.1039/C2JM34741E

[42] A. Gromov, S. Dittmer, J. Svensson, O.A. Nerushev, S.A. Perez-García, L. Licea-Jiménez, R. Rychwalski, E.E.B. Campbell, Covalent amino-functionalisation of single-wall carbon nanotubes, Journal of Materials Chemistry 15 (2005) 3334-3339. https://doi.org/10.1039/B504282H

[43] D. Berman, A. Erdemir, A.V. Sumant, Reduced wear and friction enabled by graphene layers on sliding steel surfaces in dry nitrogen, Carbon 59 (2013) 167-175. https://doi.org/10.1016/j.carbon.2013.03.006